

## Near-infrared spectroscopy for burning plasma diagnostic applications<sup>a)</sup>

V. A. Soukhanovskii

*Lawrence Livermore National Laboratory, Livermore, California 94550, USA*

(Presented 15 May 2008; received 13 May 2008; accepted 30 June 2008;  
published online 31 October 2008)

Ultraviolet and visible (UV-VIS, 200–750 nm) atomic spectroscopy of neutral and ionized fuel species (H, D, T, and Li) and impurities (e.g., He, Be, C, and W) is a key element of plasma control and diagnosis on International Thermonuclear Experimental Reactor and future magnetically confined burning plasma experiments (BPXs). Spectroscopic diagnostic implementation and performance issues that arise in the BPX harsh nuclear environment in the UV-VIS range, e.g., degradation of first mirror reflectivity under charge-exchange atom bombardment (erosion) and impurity deposition, permanent and dynamic loss of window, and optical fiber transmission under intense neutron and  $\gamma$ -ray fluxes, are either absent or not as severe in the near-infrared (NIR, 750–2000 nm) range. An initial survey of NIR diagnostic applications has been undertaken on the National Spherical Torus Experiment. It is demonstrated that NIR spectroscopy can be used for machine protection and plasma control applications, as well as contribute to plasma performance evaluation and physics studies. Emission intensity estimates demonstrate that NIR measurements are possible in the BPX plasma operating parameter range. Complications in the NIR range due to the parasitic background emissions are expected to occur at very high plasma densities, low impurity densities, and at high plasma-facing component temperatures. © 2008 American Institute of Physics. [DOI: [10.1063/1.2964230](https://doi.org/10.1063/1.2964230)]

### I. INTRODUCTION

Atomic spectroscopy in the ultraviolet (200–400 nm) and visible (400–750 nm) ranges, referred henceforth as UV-VIS spectroscopy, is one of the key elements of plasma control and diagnosis in present and near-future fusion devices, such as the International Thermonuclear Experimental Reactor (ITER).<sup>1,2</sup> The UV-VIS spectroscopic applications include detection and analysis of emission from bound-bound and free-bound transitions of neutral atoms and ions of fuel species and impurities, as well as bremsstrahlung emission due to free-free transitions.<sup>3</sup> These emissions come from hot core plasmas, the edge (pedestal) region, and plasma-wall interaction regions [scrape-off layer (SOL), divertors, and limiters]. Two main roles are envisioned for UV-VIS spectroscopic diagnostics on ITER and future magnetically confined fusion (MCF) plasma devices: (1) machine protection, basic, and advanced plasma control applications, and (2) performance evaluation and physics studies.<sup>1,4,5</sup>

A harsh nuclear environment of future MCF devices poses severe challenges to spectroscopic diagnostics. In these devices, the diagnostics will be situated in remote locations behind radiation shields. Conceptually, a typical spectroscopic diagnostic is comprised of plasma-facing mirrors, vacuum interface windows, and optical signal relay

elements, i.e., mirrors, lenses, and optical fibers, situated either in a diagnostic port plug or in a neutron-shielding labyrinth. A detection system can be placed in the port plug with adequate radiation shielding or in a diagnostic hall adjacent to the shielding labyrinth.<sup>6–8</sup>

A significant effort has been dedicated to studying diagnostic requirements in the harsh ITER environment.<sup>9</sup> A reactor-relevant diagnostic experience has been obtained in the DT operation phases of the TFTR and JET tokamaks, as well as in dedicated laboratory irradiation tests.<sup>10–12</sup> These efforts highlighted a number of diagnostic implementation and performance issues for UV-VIS spectroscopy, namely, the severe degradation of optical elements under high plasma particle, neutron, and  $\gamma$ -ray fluxes. An alternative approach proposed here avoids most of the UV-VIS spectroscopy diagnostic issues.

We propose near-infrared (NIR, 750–2000 nm) spectroscopy as a complementary diagnostic technique for plasma control and performance measurements in the burning plasma experiment (BPX) environment. Whereas the NIR spectroscopic systems share diagnostic concepts with the UV-VIS spectroscopy, optical material and component properties are much more tolerant to radiation and plasma effects in the NIR range, and a number of NIR signal extraction techniques are available at present. Since the BPX diagnostic issues are rarely faced in existing fusion plasma devices, few NIR measurements have been reported.<sup>3,13,14</sup> We present an initial study of the scope and feasibility of passive NIR spectroscopic measurements in an ITER-like environment.

<sup>a)</sup> Contributed paper, published as part of the Proceedings of the 17th Topical Conference on High-Temperature Plasma Diagnostics, Albuquerque, New Mexico, May 2008.

## II. OPTICAL MATERIALS AND COMPONENTS

Recent diagnostic reviews<sup>2,9,12</sup> have summarized the status and requirements for various spectroscopic system components with respect to radiation effects. In ITER, neutron fluxes are expected to be close to  $3 \times 10^{18} \text{ m}^{-2} \text{ s}^{-1}$  at the first wall, the dose rate  $2000 \text{ Gy s}^{-1}$ , and the neutron heating rate  $1 \text{ MW m}^{-3}$ .<sup>7</sup> Charge-exchange atomic fluxes with energies up to 1–3 keV are expected to reach  $2 \times 10^{19} \text{ m}^{-2} \text{ s}^{-1}$ . The degradation of material properties in this environment is of specific concern for BPX spectroscopic diagnostics, as a number of optical materials and techniques are under consideration for both VIS and NIR measurements. Existing data on first mirror, window, and fiber performance under harsh radiation and particle fluxes demonstrate that measurements in the NIR range have clear advantages over those in the UV-VIS range.

*a. Mirrors.* Optical properties of first mirrors, such as reflectivity and polarization, degrade upon exposure of the mirror surface to plasma particle fluxes. Two main mechanisms of surface degradation have been identified—surface erosion and material deposition. Erosion depths and deposition layers of tens of nanometers are expected in ITER. The specular reflectance is a function of the wavelength  $\lambda$  and mean surface roughness  $d$ . The total reflectivity  $R$  is described by the Benett formula,<sup>15</sup>

$$R = R_0 e^{-(4\pi d)^2/\lambda^2}. \quad (1)$$

In the NIR region,  $R$  is higher by up to 30% for the same surface roughness, or alternatively, similar reflectivity degradation in NIR and UV is caused by roughnesses that differ by 80% in size, according to Eq. (1). Recent tests indicated that mirror heating could prevent or slow down both the erosion and deposition in a deposition-dominated environment, where without heating, the total reflectivity of Mo mirrors was reduced from  $\sim 60\%$  to  $5\%$ – $40\%$  in the UV-VIS range, and from  $60\%$ – $90\%$  by only  $2\%$ – $10\%$  in the NIR range.<sup>16</sup> In an erosion-dominated environment, the use of special materials (Mo, W, Rh, Cu, and stainless steel) and manufacturing techniques (single crystal mirrors and polycrystalline mirrors) has been shown to slow down reflectivity degradation in the UV-VIS range. No degradation was detected in the NIR range,<sup>17</sup> where high reflectivity coefficients for all candidate mirror materials were predicted and measured.

*b. Windows and lenses.* Radiation-induced damage of bulk optical materials is due to the atomic displacement effects and electronic excitation effects. The accumulated damage, caused by radiation-induced absorption (RIA), leads to a permanent optical transmission loss. The dynamic losses are due to the radiation-induced luminescence (RIL) and Cherenkov radiation. Candidate ITER materials, such as quartz and fused silica, show both RIA and RIL in the UV-VIS range, and no adverse effects in the NIR range. The Cherenkov radiation intensity is an irreducible source of background luminescence. Because its intensity is proportional to  $1/\lambda^2$ , it decreases rapidly in the NIR range.<sup>11</sup>

*c. Fibers.* Optical fibers are considered a more attractive option for signal relay elements than mirrors and lenses because they simplify optical design and alignment procedures,

as well as realize significant cost and space savings. Optical fiber materials are also subject to RIA, RIL, and Cherenkov radiation. Key parameters for radiation-resistant fibers are dopant elements, OH-content, presence of impurity elements, cladding type, fabrication mechanism, and preconditioning techniques. Recent technology efforts resulted in a number of radiation-resistant fiber candidates with OH-doped and F-doped fused silica  $\text{SiO}_2$  cores, as well as mitigation techniques, such as the hydrogen treatment during fabrication and heat treatment.<sup>18</sup> Candidate ITER fiber materials, the KU1 and KS4V types of fused silica, show significant resilience to radiation effects in the VIS range. All spectrally resolved radiation effect measurements show that these and other fibers (e.g., quartz and sapphire) are practically free of any RIA and RIL in the NIR range. Finally, an attractive candidate for a fiber-based relay element is the hollow fiber that transmits exclusively in the NIR range.<sup>19</sup>

*d. Detectors.* Present day spectroscopic techniques can be used for NIR diagnostics, since instruments and detectors are to be located behind radiation shields. The NIR techniques are conceptually similar to UV-VIS spectroscopy,<sup>3</sup> and may include Czerny–Turner spectrometers, filtered photodiode detectors and cameras, build from commercially available components. Since the response of silicon-based charge-coupled devices (CCDs) and photodiodes is limited to the region below 1100 nm, other detector materials, such as Ge, PbS, InAs, InGaAs, and PbSe, are used in NIR.

## III. DIAGNOSTIC SCOPE

A brief review of the UV-VIS spectroscopy issues in the harsh nuclear environment (Sec. II) demonstrated clear advantages of NIR measurements. Following Ref. 4, we now discuss how NIR spectroscopy can address the diagnostic, plasma control, and machine protection goals envisioned for UV-VIS spectroscopy. The basic tasks include H/D/T- $\alpha$  measurements for ELM and L-H transition monitoring, impurity influx monitoring, and measurements of  $Z_{\text{eff}}$ . The advanced applications encompass Doppler shift and Doppler

TABLE I. Candidate NIR measurements for BPX machine protection, control, and physics studies.

Measurement	NIR Candidate
ELMs, L-H transition	$P_{\alpha}$ , $P_{\beta}$ lines
H, D, T influx and recycling profiles in SOL and divertor	$P_{\alpha}$ , $P_{\beta}$ lines
H/D/T fuel ratio	$P_{\alpha}$ , $P_{\beta}$ lines
Recombination monitoring, $T_e$ and $n_e$ in recombining Divertor	Stark broadening of D/T and He I, He II series lines
Divertor and SOL He density	He I, He II lines
Impurity influx and profiles in SOL and divertor	Li, Be, C, N, O lines Ne, Ar, Kr lines W, Mo lines
SOL and divertor flows and passive $T_i$	Doppler shift and broadening of impurity lines above
$Z_{\text{eff}}$	NIR bremsstrahlung
Corresponding edge measurements	As above

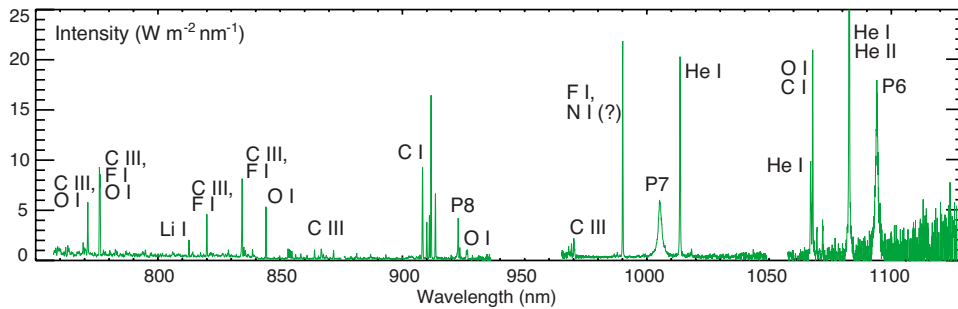


FIG. 1. (Color online) Survey divertor spectra measured in 0.7 MA, 4 MW NBI-heated NSTX plasmas.

broadening spectroscopies, charge-exchange spectroscopy, and Stark broadening spectroscopy for rotation, flow, ion, and impurity species density  $n_{i,Z}$  and temperature  $T_i$  profile, effective plasma charge  $Z_{\text{eff}}$  profile, and divertor  $T_e$  and  $n_e$  measurements, as well as fuel ratio and neutral density measurements. The proposed NIR measurements are summarized in Table I.

An initial survey of possible NIR applications has been performed in the National Spherical Torus Experiment (NSTX), a midsize mega-Ampere-class fusion plasma device with lithium and carbon plasma-facing components (PFCs), up to 6 MW deuterium heating beams and up to 6 MW of high-harmonic fast wave heating.<sup>20</sup> In the survey, a commercial 0.5 m Czerny–Turner spectrometer equipped with a CCD detector and a commercial NIR edge filter (Edmunds Optical R72) were used.<sup>21</sup> Both the spectrometer and the fiber-optic imaging system were designed for UV-VIS measurements, thereby limiting the useful wavelength range to about 1150 nm.

A survey spectrum from the NSTX lower divertor is shown in Fig. 1. The survey was composed of the spectra taken in five reproducible 0.7 MA, 4 MW NBI-heated discharges. Besides the atomic deuterium Paschen series lines  $n=3-m$ , where  $m=6-8$ , the lines identified in NSTX spectra are attributed to low- $Z$  impurities. In particular, several bright He I, He II, N I, and O I–II are visible. As for carbon lines, only C I and C III lines were identified. Further tokamak work on line detection and identification in the region is needed. Ionization per photon (SX/B) factors are available in the ADAS system<sup>22</sup> for many of the lines, making them good candidates for particle influx measurements.

While the region  $\lambda \leq 910$  nm contains many small atomic and molecular lines, few lines can be seen in the range  $\lambda=910-1100$  nm. The line emission-free regions are candidates for NIR bremsstrahlung measurements for plasma  $Z_{\text{eff}}$  analysis, as has been shown in Refs. 23 and 24, if wall reflections and thermal background emission can be neglected.

To illustrate the complementarity of UV-VIS and NIR measurements, brightness time histories of divertor deuterium Balmer- $\gamma$  (434 nm) and Paschen- $\gamma$  (1094 nm) lines are compared in Fig. 2. Both lines were measured in the same divertor region. The visible line was measured with a filterscope<sup>25</sup> consisting of a PMT detector, a narrow-bandpass ( $\Delta\lambda=1.5$  nm) interference filter, and a 5 kHz bandwidth amplifier. The NIR line was measured with the spectrometer at a CCD framing rate of 25 Hz. Both diagnostics were calibrated *in situ* using an integrating sphere calibration transfer standard. A constant low ratio between the two line intensities  $R_{B,\gamma/P,\gamma} \approx 6$  indicates that same atomic processes are responsible for populating the upper levels of these transitions. According to ADAS calculations, the ratios of  $R_{B,\gamma/P,\gamma} = 5-11$  ( $T_e=1-50$  eV) are obtained in ionizing plasmas, and about 2 in recombining plasmas.

Estimates of plasma  $T_e$  and  $n_e$  in a detached divertor can be obtained from hydrogenic series line emission spectra and photorecombination continuum slope.<sup>26</sup> Substantial Stark broadening ( $\lambda/\Delta\lambda \approx 300$ ) of the high- $n$  Paschen series lines, due to plasma electron and ion microfields, makes them good candidates for  $n_e$  measurements in the range  $5 \times 10^{19}-10^{22} \text{ m}^{-3}$ .<sup>21,27</sup> Shown in Fig. 3 are the Paschen P8–P11 NIR lines measured in the recombining divertor in

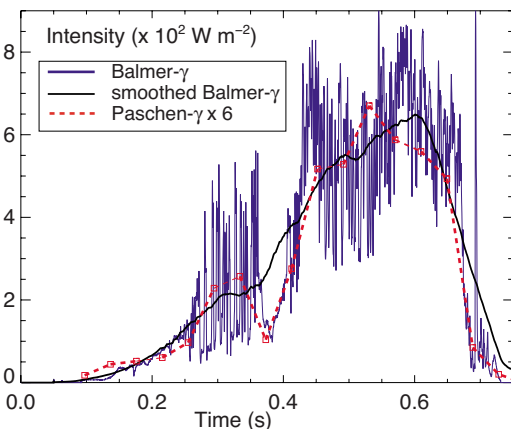


FIG. 2. (Color online) Time histories of Balmer- $\gamma$  (2–5) and Paschen- $\gamma$  (3–6) line intensities in the NSTX divertor.

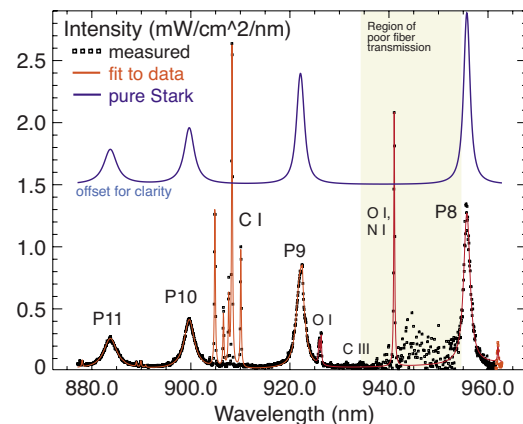


FIG. 3. (Color online) Stark broadening of P8–P11 Paschen series lines in the recombining (detached) divertor.

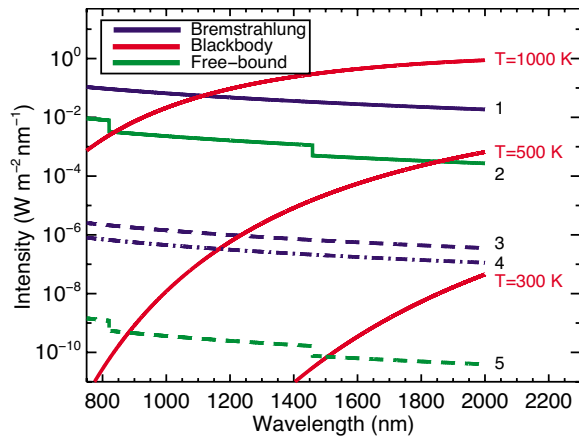


FIG. 4. (Color online) NIR intensities of thermal (blackbody) emission, bremsstrahlung emission, and free-bound hydrogen emission. Parameters are as follows: lines 1,2— $T_e=5$  eV,  $n_e=5 \times 10^{20} \text{ m}^{-3}$ ,  $Z_{\text{eff}}=2.5$ ; lines 3,5— $T_e=1000$  eV,  $n_e=1 \times 10^{19} \text{ m}^{-3}$ ,  $Z_{\text{eff}}=1.5$ ; line 4— $T_e=10\,000$  eV,  $n_e=1 \times 10^{19} \text{ m}^{-3}$ ,  $Z_{\text{eff}}=1.5$ .

NSTX. Average densities in the range  $n_e \approx (2.5-3.5) \times 10^{20} \text{ m}^{-3}$  were inferred from the Stark broadening analysis of the lines.<sup>21</sup>

The discussed examples demonstrate that a number of NIR measurements are possible; however, more work is needed on present day devices to bring the NIR spectroscopy to the level of maturity of the UV-VIS spectroscopy.<sup>3</sup>

**IV. EMISSION INTENSITY ESTIMATES**

Reliable measurements of spectral line intensities and profiles are only possible when the background emission intensity is low. The NIR signal contamination comes from three sources: thermal emission from PFC surfaces, plasma bremsstrahlung emission, and emission due to the free-bound transitions (recombination emission). To demonstrate the feasibility of NIR line emission measurements, estimates of line and background intensities are discussed in this section.

Example calculations of the background emission are shown in Fig. 4. In the examples, a line of sight integration of emissivities  $\epsilon$  through a 1 m isothermal plasma was per-

formed. The bremsstrahlung intensity was estimated using the approach from Ref. 25. Plasma parameters for these estimates were chosen to determine typical high and low levels of  $\epsilon_{\text{brem}} \sim n_e^2 Z_{\text{eff}} T_e^{-1/2}$ . Thermal emission was calculated using Planck’s blackbody emissivity formula. The free-bound hydrogenic intensity was calculated using the CHIANTI suite of codes.<sup>28</sup> Typical line intensities are expected to be in the range 0.01–1000  $\text{W m}^{-2} \text{ nm}^{-1}$ . The thermal emission intensity becomes appreciable only at high PFC temperatures  $T \geq 1000$  K, e.g., in “hot spots.” The free-bound emission intensity can also generally be neglected. The bremsstrahlung emission starts competing with line emission only at very high densities and high  $Z_{\text{eff}}$  levels, marginally achievable in BPX.<sup>5</sup> Overall, it appears that the NIR background intensity at the BPX plasma parameters is sufficiently low to allow reliable line emission measurements.

To provide further comparison of the bremsstrahlung and line intensities, we calculated the latter for three candidate NIR lines: hydrogen  $P_\alpha$  ( $\lambda=1875.6$  nm,  $n=3-4$ ), Be II ( $\lambda=948$  nm), and C III ( $\lambda=970.3$  nm) using atomic data from the ADAS database<sup>22</sup> (Fig. 5). These calculations follow the methodology of Ref. 29 where a design for the ITER divertor impurity monitor was evaluated. Line intensities were calculated for a range of  $T_e$  and  $n_e$ , and divertor particle flux rates expected in ITER.<sup>29</sup> The conclusion for NIR line intensities is similar to the UV-VIS situation:<sup>29</sup> difficulties may be encountered at very high electron densities, where bremsstrahlung and free-bound emission become appreciable, and at low recycling and impurity influx levels, where line intensities become low.

**V. DISCUSSION**

A conceptual evaluation of NIR spectroscopic diagnostic applications in the harsh BPX nuclear environment demonstrate that (1) optical material and component properties under intense neutron,  $\gamma$ -ray, and plasma fluxes favor measurements in the NIR range, and (2) NIR measurements can fully address machine protection, control, and physics studies

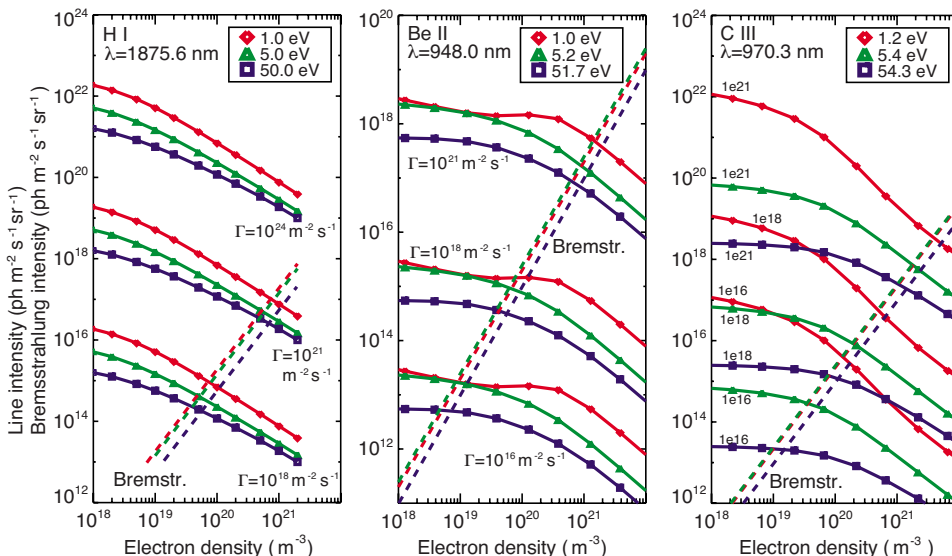


FIG. 5. (Color online) Line intensities of hydrogen Paschen- $\alpha$  at 1875.6 nm, Be II line at 948.0 nm, and C III line at 970.3 nm as functions of density and particle flux.

goals defined for UV-VIS spectroscopy. Intensity estimates demonstrate that NIR measurements are possible in the operating parameter range of BPX plasmas.

To promote the concept of NIR spectroscopic measurements in the BPX environment further, a number of issues, common to both UV-VIS and NIR diagnostics, still need to be addressed. They include (1) wall reflections (e.g., Ref. 30), expected to be higher in the NIR range, (2) molecular band emission, and (3) for graphite PFCs, the background carbon luminescence.<sup>31</sup>

Finally, active NIR spectroscopy is an attractive possibility. The motional Stark effect and beam emission spectroscopy measurements are probably not possible in the NIR range, because of a prohibitively large number of deuterium atom states involved at  $n=3,4$ . However, NIR charge-exchange recombination spectroscopy should be considered since a number of suitable transitions between high  $n$  levels in highly ionized impurities (He II, Be V, C VI, and Ne X) exist.

## ACKNOWLEDGMENTS

Collaboration with Dr. R. Kaita and Dr. A. L. Roquemore (PPPL) is acknowledged. The entire NSTX team is acknowledged for software, engineering, and technical support, as well as for plasma, NBI, and diagnostic operations. ADAS was used through the ORNL Controlled Fusion Atomic Data Center (CFADC). CHIANTI is a collaborative project involving the NRL (Washington, DC), RAL (UK), MSSL (UK), the Universities of Florence (Italy), and Cambridge (UK), and George Mason University (Fairfax, VA). This work was performed under the auspices of the U.S. Department of Energy under Contract Nos. W-7405-Eng-48, DE-AC52-07NA27344, and DE-AC02-76CH03073.

<sup>1</sup>K. Young, A. Costley, R. Bartiromo, L. De Kock, E. Marmor, V. Mukhovatov, K. Muraoka, A. Nagashima, M. Petrov, P. Stott *et al.*, *Nucl. Fusion* **39**, 2541 (1999).

<sup>2</sup>A. Donne, A. Costley, R. Barnsley, H. Bindslev, R. Boivin, G. Conway, R. Fisher, R. Giannella, H. Hartfuss, M. von Hellermann *et al.*, *Nucl. Fusion* **47**, 337 (2007).

<sup>3</sup>B. C. Stratton, *Fusion Sci. Technol.* **53**, 431 (2008).

<sup>4</sup>T. Sugie, A. Costley, A. Malaquias, and C. Walker, *J. Plasma Fusion Res.* **79**, 1051 (2003).

<sup>5</sup>K. M. Young, *Fusion Sci. Technol.* **53**, 281 (2008).

<sup>6</sup>C. Walker, R. Barnsley, A. Costley, R. Gottfried, B. Haist, K. Itami, T. Kondoh, G. Loesser, J. Palmer, T. Sugie *et al.*, *Fusion Eng. Des.* **74**, 685 (2005).

<sup>7</sup>A. E. Costley, T. Sugie, G. Vayakis, and C. I. Walker, *Fusion Eng. Des.* **74**, 109 (2005).

<sup>8</sup>D. W. Johnson and A. E. Costley, *Fusion Sci. Technol.* **53**, 751 (2008).

<sup>9</sup>G. Vayakis, E. R. Hodgson, V. Voitsenya, and C. I. Walker, *Fusion Sci. Technol.* **53**, 699 (2008).

<sup>10</sup>A. Ramsey, *Rev. Sci. Instrum.* **66**, 871 (1995).

<sup>11</sup>A. C. Maas, P. Andrew, P. Coad, A. Edwards, J. Ehrenberg *et al.*, *Fusion Eng. Des.* **47**, 247 (1999).

<sup>12</sup>T. Shikama, *Nucl. Fusion* **43**, 517 (2003).

<sup>13</sup>A. Meigs, G. McCracken, C. Maggi, R. Monk, L. Horton, M. von Hellermann, M. Stamp, and P. Breger, Proceedings of 27th EPS Conference on Controlled Fusion and Plasma Physics, Budapest, Hungary, 2000, Vol. ECA 24B, pp. 1264–1267.

<sup>14</sup>I. Furno and G. A. Wurden, *Rev. Sci. Instrum.* **75**, 4112 (2004).

<sup>15</sup>V. Voitsenya, A. Costley, V. Bandourko, A. Bardamid, V. Bondarenko, Y. Hirooka, S. Kasai, N. Klassen, V. Konovalov, M. Nagatsu *et al.*, *Rev. Sci. Instrum.* **72**, 475 (2001).

<sup>16</sup>D. L. Rudakov, J. A. Boedo, R. A. Moyer, and A. Litnovsky, *Rev. Sci. Instrum.* **77**, 10F126 (2006).

<sup>17</sup>A. Litnovsky, V. Voitsenya, A. Costley, and A. Donne, *Nucl. Fusion* **47**, 833 (2007).

<sup>18</sup>M. Decretton, T. Shikama, and E. Hodgson, *J. Nucl. Mater.* **329**, 125 (2004).

<sup>19</sup>C. M. Smith, N. Venkataraman, M. T. Gallagher, and D. Muller, *Nature (London)* **424**, 657 (2003).

<sup>20</sup>M. Ono, S. Kaye, Y.-K. Peng, G. Barnes, W. Blanchard, M. Carter, J. Chrzanowski, L. Dudek, R. Ewig, D. Gates *et al.*, *Nucl. Fusion* **40**, 557 (2000).

<sup>21</sup>V. A. Soukhanovskii, D. W. Johnson, R. Kaita, and A. Roquemore, *Rev. Sci. Instrum.* **77**, 10F127 (2006).

<sup>22</sup>H. P. Summers, The ADAS User Manual, version 2.6, <http://adas.phys.strath.ac.uk>, 2004.

<sup>23</sup>K. H. Steuer, H. Rohr, and B. Kurzan, *Rev. Sci. Instrum.* **61**, 3084 (1990).

<sup>24</sup>F. Orsitto, M. R. Belforte, A. Brusadin, E. Giovannozzi, D. Pacella, and M. J. May, *Rev. Sci. Instrum.* **70**, 925 (1999).

<sup>25</sup>A. T. Ramsey and S. L. Turner, *Rev. Sci. Instrum.* **58**, 1211 (1987).

<sup>26</sup>J. L. Terry, B. Lipschultz, A. Y. Pigarov, S. I. Krashennnikov, B. Labombard, D. Lumma, H. Ohkawa, D. Pappas, and M. Umansky, *Phys. Plasmas* **5**, 1759 (1998).

<sup>27</sup>B. Welch, H. Griem, J. Weaver, J. Brill, J. Terry, B. Lipschultz, D. Lumma, G. McCracken, S. Ferri, A. Calisti *et al.*, *AIP Conf. Proc.* **386**, 113 (1997).

<sup>28</sup>E. Landi, M. Landini, K. P. Dere, P. R. Young, and H. E. Mason, *Astron. Astrophys. Suppl. Ser.* **135**, 339 (1999).

<sup>29</sup>T. Sugie, H. Ogawa, T. Nishitani, S. Kasai, J. Katsunuma, M. Maruo, K. Ebisawa, T. Ando, and Y. Kita, *Rev. Sci. Instrum.* **70**, 351 (1999).

<sup>30</sup>E. M. Hollmann, A. Y. Pigarov, and R. P. Doerner, *Rev. Sci. Instrum.* **74**, 3984 (2003).

<sup>31</sup>E. Delchambre, R. Reichle, R. Mitteau, N. Missirlian, and P. Roubin, *J. Nucl. Mater.* **337–339**, 1069 (2005).